

19

**Evaluation Of The Possibility Of Using Ultrasound For The
Remediation Of A Sandy Aquifer Polluted By
Light Nonaqueous Phase (LNAPL).**

Case Study: Fuel Spill 12 at the Massachusetts

Military Reservation

by

Jacques de Lalaing

Submitted to the
department of civil and environmental engineering in partial fulfillment
of the requirements for the degree of

MASTER OF ENGINEERING
in civil and environmental engineering

at the

MASSACHUSETTS INSTITUTE OF TECHNOLOGY

June, 1997

© 1997 Massachusetts Institute of Technology. All Rights Reserved

The Author hereby grants to MIT permission to reproduce and to distribute publicly paper and
electronic copies of this thesis document in whole and in part.

Signature of the author.....

Department of Civil and Environmental Engineering
May 9, 1996

Certified by.....

Harold Hemond
Professor of Civil and Environmental Engineering

Accepted by.....

Joseph M. Sussman
Chairman, Department Committee on Graduate Studies

241997

**Evaluation Of The Possibility Of Using Ultrasound For The Remediation Of A
Sandy Aquifer Polluted by Light Nonaqueous Phase Liquid (LNAPL).
Case Study: Fuel Spill 12 at the Massachusetts Military Reservation**

by

Jacques de Lalaing

Submitted to the Department of Civil and Environmental Engineering
on May 9, 1996 in partial fulfillment of the requirements of the degree of
Master of Engineering in Civil and Environmental Engineering

ABSTRACT

Over the past fifty years, LNAPL pollution of subsurface environments has become one of the most pressing threat to the national water resources. Most of the LNAPL spill originate from faulty storage tanks or leaking pipeline and from accidents involving tank trucks and railroad cars. Although, in general, the volume involved at any particular sites is small, the frequency of occurrence and widespread distribution of such incidents are cause for concern. On a national level, the EPA investigates over 1000 large hydrocarbon spills every year. All of these present a direct threat to the environment and to the local water resources. The multiplicity of exposure routes - direct human exposure (inhalation, skin contact, ingestion) and indirect exposure (ingestion of contaminated food, water...) - makes LNAPL pollution a direct danger to the human health.

The remediation of LNAPL polluted subsurface is a strong priority in the EPA ranking. Unfortunately, the state of the art technologies used today, while being very costly and time consuming, are not very efficient. While the need for innovative technologies is recognized by both the public and private sectors, few new techniques have been widely developed and implemented. This study examines the possibilities presented by the use of ultrasound in subsurface in-situ remediation.

Ultrasound can be used on two levels for the clean up of a site.

- Improve the free phase pumping by easing the movement of LNAPL to the surface of the aquifer. First, through emulsification of the organic phase, and, second, by inducing transient change in pore geometry through vibration, thereby allowing the LNAPL to flow to the surface by buoyancy.
- Induce the breakdown of the dissolved organics through the use of cavitation. Cavitation refers to the formation and collapse of microbubble that take place in liquids irradiated by a strong ultrasound beam. The high temperature and pressures (1000 atm, 5000 ° K) obtained during the collapse of the microbubbles can induce the decomposition of dissolved organics into CO₂, H₂O, and other primary components.

Acknowledgments

I would first like to thank my family for the love and support I have received throughout my life, and for allowing me to come to MIT to pursue my education. It has been hard to be away from home for so long but it has worth it.

I would also like to thank my advisor, Professor Harry Hemond, for taking the time out of his busy schedule to support and guide me during my research. His insight and knowledge have been invaluable in keeping me on track during this project.

I would like to thank Bruce Jacobs and Pete Shanahan for their help and patience in following us through the long process of writing a thesis.

And last but not least I would like to thank “Les Mousquetaires” for their unwavering friendship. They kept me smiling through this nine month marathon called the M.Eng.

This thesis is a partial fulfillment of a class in the Master of Engineering Program in Environmental Engineering in the Department of Civil and Environmental Engineering at the Massachusetts Institute of Technology. This research contributed to a group project which evaluated the present and potential remediation schemes used at a fuel spill site at the Massachusetts Military Reservation on Cape Cod. The other team members are Dan Baker, Ronald Lee, Dave Lockwood, Yervant Vichibian and Scott Goddard. The group project was the compilation of each of the individual group thesis.

Table of Content

1. Introduction to the Fuel Spill 12	6
2. FS-12 Site Description	9
2.1 Physical Characteristics.....	9
2.1.1 Location	9
2.1.2 Topography and Geology	9
2.1.3 Regional Climate	11
2.1.4 Ecosystems.....	11
2.2 Demographics and Socio-Economic Impacts	11
2.3 Historical Site Activity.....	12
2.3.1 Military Activity.....	12
2.3.2 Regulation	12
2.3.3 History of The Contamination And Cleanup-Up Efforts	12
3. Fuel Spill 12 Description	14
3.1 Physical Characteristics.....	14
3.1.1 Geology.....	14
3.1.2 Hydrogeology.....	15
3.2 Remedial Activities.....	16
3.2.1 Plume Containment.....	16
3.2.2 Source Remediation.....	16
4. Natural movement of LNAPL in the saturated and unsaturated soils	18

4.1.1 The unsaturated zone.....	19
4.1.2 The capillary zone.....	21
4.1.3 The saturated zone.....	22
5. Mechanism of LNAPL trapping in the saturated zone.....	23
5.1 Snap-off.....	23
5.2 By-passing.....	25
6. Sound Waves And Ultrasounds For The Mobilization Of LNAPL.....	27
7. Background on the physics of ultrasound.....	30
7.1 The production of sound wave and ultrasound.....	30
7.2 Propagation and physics of cavitation.....	33
7.2.1 Ultrasound propagation.....	33
7.2.2 Cavitation.....	34
8. Effects of ultrasound on LNAPL in water.....	41
8.1 Molecular scale effects of the ultrasounds on LNAPL in water.....	41
8.1.1 Effects of the ultrasounds on the chemical breakdown of LNAPL in water.....	41
8.1.2 Emulsification by ultrasound irradiation.....	43
8.2 Effects of vibration on LNAPL mobilization.....	46
9. Conclusion.....	48
10. Reference.....	49

Table of Figures

FIGURE 1: MMR PLUME MAP	8
FIGURE 2: LOCATION OF THE MMR.....	10
FIGURE 3: HYDROLOGY AT THE MMR	15
FIGURE 4: AN OIL SEEPAGE SCHEMATIC	19
FIGURE 5: CONTAMINATION TRANSPORT THROUGH UNSATURATED HOMOGENEOUS AND HETEROGENEOUS SOILS	20
FIGURE 6: WETTING FLUID DISPLACING A NON-WETTING FLUID FROM A CIRCULAR, HIGH ASPECT RATIO PORE UNDER STRONGLY WET CONDITIONS.	24
FIGURE 7: LOW WETTING CONDITION.....	24
FIGURE 8: EFFECT OF PORE ASPECT RATIO ON LNAPL TRAPPING.....	25
FIGURE 9: BY-PASS TRAPPING USING THE PORE DOUBLET MODEL.	26
FIGURE 10: PIEZOELECTRIC TRANSDUCER.....	31
FIGURE 11: MAGNETOSTRICTION TRANSDUCER.....	32
FIGURE 12: VARIATION OF THRESHOLD INTENSITY WITH FREQUENCY OF WATER AT ROOM TEMPERATURE	37
FIGURE 13: MICROBUBBLES (10^{-6} CM) ATTACHED TO FREE FLOATING DUST PARTICLES (5×10^{-5} CM).....	40
FIGURE 14: TIME PROFILES OF FIVE CHLORINATED HYDROCARBONS BY ULTRASONIC IRRADIATION	42
FIGURE 15: TIME PROFILE OF DEGRADATION OF TRICHLOROETHYLENE AND TRANSFORMATION OF PRODUCTS UNDER ARGON.	42
FIGURE 16: MICROSTREAMING IN THE VICINITY OF OSCILLATING AIR BUBBLES; V IS THE PARTICLE VELOCITY OF THE BUBBLE SURFACE.	44
FIGURE 17: EFFECTS OF EMULSIFICATION OF LNAPL MOBILIZATION.....	45
FIGURE 18: THEORETICAL VARIATION OF THE MAXIMUM LENGTH OF STABLE GANGLION WITH RESPECT TO PORE THROAT DIAMETER UNDER (A) VISCOUS CONDITIONS; AND (B) BUOYANCY CONDITIONS.....	47
FIGURE 19: HYPOTHESIZED CHANGES IN GANGLION GEOMETRY :(A) STABLE GANGLION UNDER STATIC CONDITIONS; (B) ELONGATED GANGLION DUE TO CHANGE IN PORE STRUCTURE UNDER BUOYANCY PRESSURE ALONE; AND (C) SPLIT GANGLION DUE TO CHANGE IN PORE STRUCTURE UNDER VISCOUS PRESSURE	47

1. Introduction to the Fuel Spill 12

Fuel Spill 12 (FS-12) is one of several groundwater plumes emanating from the Massachusetts Military Reservation (MMR) on Cape Cod. Over the years, the MMR has been occupied by several different military organizations, and was particularly active during World War II. During its 86 years of operation, the MMR has been home to a number of pollution incidents, and was declared a Superfund site in 1990.

The FS-12 plumes, originate from a 70,000 gallons spill of jet fuel that leaked from an underground pipeline in 1972. They were discovered in 1990. While the leak occurred on the reservation, the majority of the plumes reside just outside the MMR perimeter (Figure 1). The contaminants of the fuel spill include benzene and ethylene dibromide (EDB), both of which are known carcinogens. These plumes pose no immediate threat to Cape Cod water resources. However, with the increase of the population, and their dependence on ground water. The continuing growth of the plume, have concerned many scientists and members of the surrounding communities.

Air sparging wells and soil vapor extraction (SVE) units are currently in operation near the source of the contamination. A pump and treat system has been designed to prevent further migration of EDB at the perimeter of the plume. These systems together, as they stand now, will not remediate the benzene or EDB plumes to acceptable contamination levels. The air sparging wells and SVE units only cover a portion of FS-12. Moreover, pilot testing for the pump and treat system has found that substantial concentrations of EDB have already passed down gradient of the perimeter of the proposed well fence.

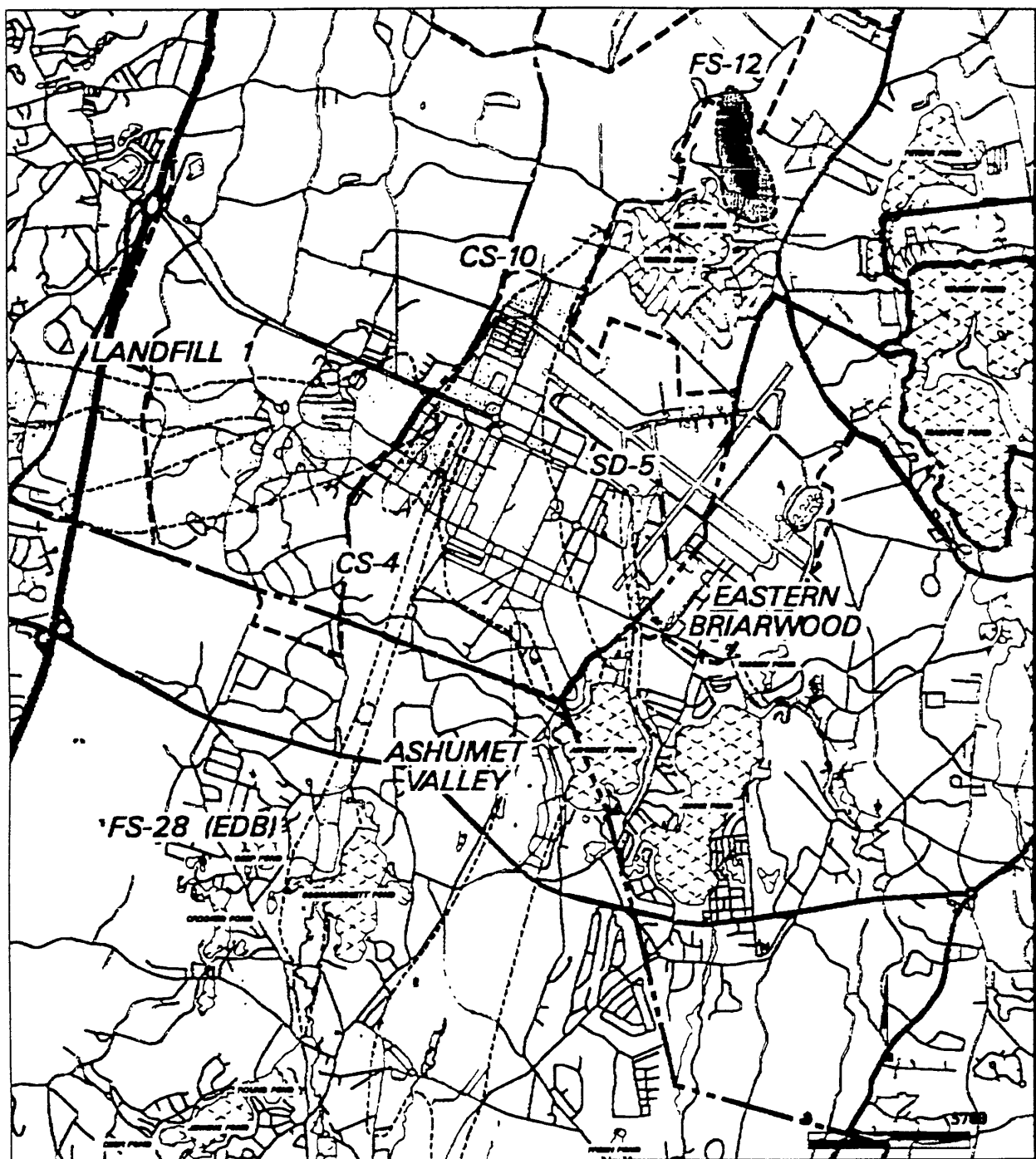


Figure 1: MMR Plume Map

2. FS-12 Site Description

2.1 Physical Characteristics

2.1.1 Location

The Massachusetts Military Reservation (MMR) is located in western Cape Cod, Massachusetts, about 60 miles south of Boston, and borders the townships of Bourne, Falmouth, Mashpee, and Sandwich (Figure 2). The military reservation consists of 22,000 acres in Barnstable County and abuts the Cape Cod Canal on its northwest end. Various facilities and related operations of the Department of Defense (DOD) branches are housed at the reservation. These operations include: U.S. Coast Guard, U.S. Marine Corps, U.S. Army National Guard (ARNG [Camp Edwards]), U.S. Air Force, and U.S. Air National Guard (ANG [Otis ANG Base]). Other portions of the base are used by the Veterans Administration National Cemetery, the U.S. Department of Agriculture, and the Commonwealth of Massachusetts. The southern portion of the reservation contains most of the facilities while the northern portion consists of several firing ranges which the ARNG uses for training with live ammunition.

2.1.2 Topography and Geology

The topography of western Cape Cod is typified by hummock hills, large areas of low relief, and marshy lowlands. The main southern section of the MMR is located within a broad, southward sloping glacial outwash plain, termed the Mashpee pitted plain (MPP). The MPP is characterized by low topographic relief and an abundance of kettle hole ponds and marshes. Several valleys transect the plain in a north to south direction. The plain is bounded to the north and west by terminal moraines where the MMR exhibits irregular, hilly terrain with greater topographic relief. Elevations range from a high of 306 feet, at Pine Hill in the west-central portion of the MMR, to a low of 0 feet at sea level.

The glacial outwash plain, which comprises most of the area of the MMR, consists of highly permeable sand and gravel, and locally occurring lenses of lower permeability, fine grained

sand, silt and clay. These sands and gravel are commonly poorly graded, medium to coarse grained sand with well graded gravel. The predominant sediments are quartz and feldspar with surface coatings of iron oxide and occasionally manganese oxide (Knoll et al., 1991). The well graded deposits of the Sandwich Moraine to the north and the Buzzards Bay Moraine to the west were deposited at the terminus of two adjacent glacial lobes during the last glacial advance and retreat. The sediments of these moraines are mixtures of till, sand, silt, clay, and gravel to boulder size clasts.

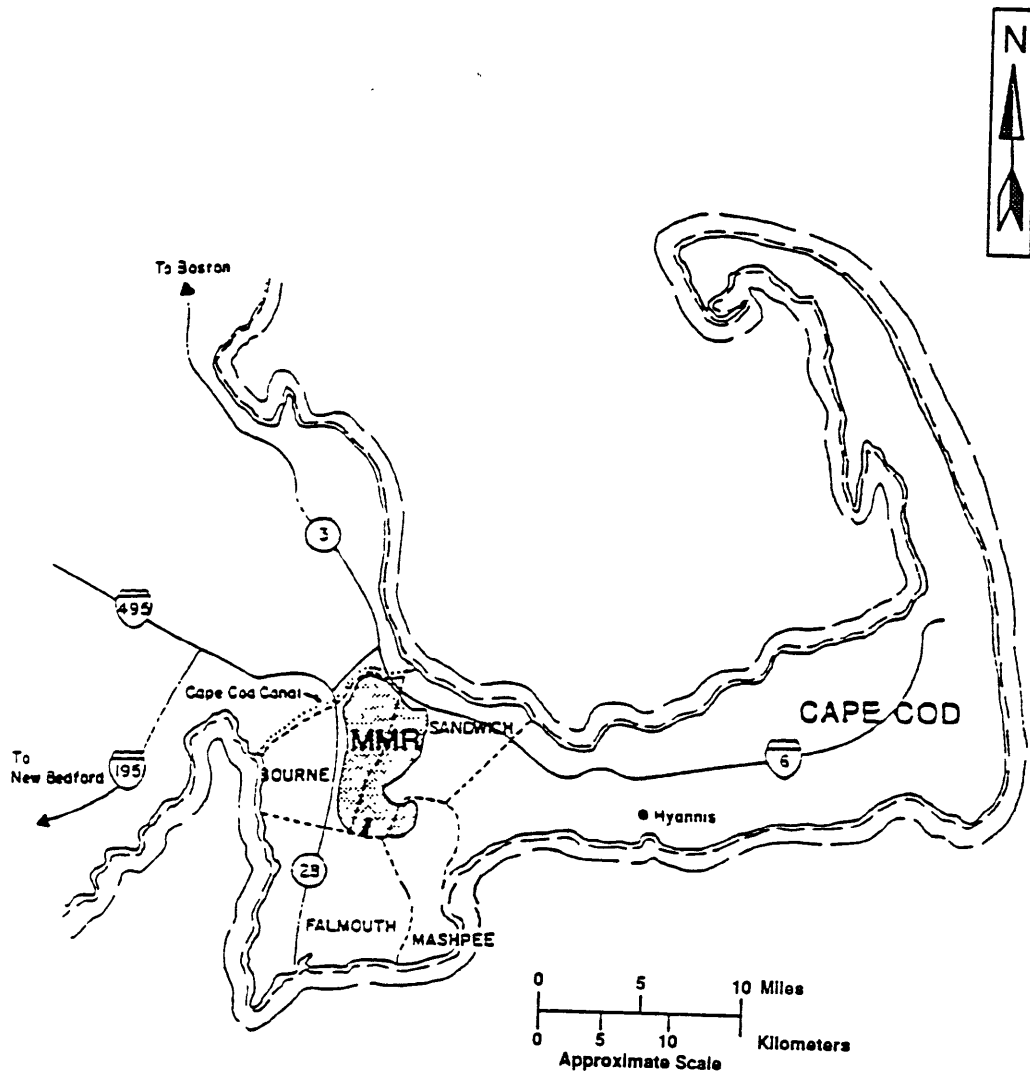


Figure 2: Location of the MMR

(Stone & Webster, 1995)

2.1.3 Regional Climate

Cape Cod has a temperate climate with an average temperature ranging from 19 to 81 degrees Fahrenheit. Temperatures remain fairly moderate due to the proximity to the Atlantic Ocean and the accompanying Gulf Stream. Wind speeds typically vary from 9 to 12 miles per hour with stronger storm velocities of 40 to 100 mph. Annual precipitation averages 48 inches with a somewhat higher portion in winter than summer. Annual groundwater recharge is in the range of 26 inches/year. The one-year/24-hour rainfall event measures 2.7 inches.

2.1.4 Ecosystems

The coastal plain ponds, formed in the glacial kettles of Cape Cod, are considered unique and sensitive natural communities by the Massachusetts Division of Fisheries and Wildlife. The rare ecosystem that develops on the shores of these ponds is highly sensitive to water level, temperature, and pH changes.

2.2 Demographics and Socio-Economic Impacts

The Fuel Spill-12 plume is located on the Upper Cape, near the top of the Sagamore lens. Being the sole-source water-supply aquifer for western Cape Cod, the lens is of vital importance to the four towns adjacent to the MMR - Falmouth, Mashpee, Sandwich, and Bourne (Ryan, 1980).

The MMR has a year round population of approximately 2,000 people with an additional 800 nonresident employees. The population of the four surrounding towns fluctuates greatly between winter (29,000) and summer (70,000) due to a strong tourism industry. Between 1980 and 1990, the Upper Cape population grew 35%. As a reference, the population growth of Massachusetts was only 5% over the same period (Bosch et al. 1996).

In the Upper Cape, 80% of the population is hooked up on a public water supply system. This amounts to an average off-season demand of 8 million gallons per day (MGD) with a peak of 16 MGD during the summer. The remaining 20% of the population relies entirely on private wells for their water supply (Bosch et al. 1996).

2.3 Historical Site Activity

2.3.1 Military Activity

The MMR has been in existence since 1912 and was a major installation for the U.S. Air Force from 1948 to 1973. Since 1973, the MMR has been used primarily by the Massachusetts National Guard and the U.S. Coast Guard. In 1986, the National Guard Bureau's Installation Restoration Program (IRP) was started to investigate contaminant plumes related to the handling of toxic and hazardous materials at the MMR (Masterson et al. 1996)

2.3.2 Regulation

The MMR was listed as a Superfund site on the National Priority List on November 21, 1989. The National Guard Bureau (NGB) and the U.S. Coast Guard entered into an Interagency Agreement (IAG) with the EPA in July 1991. As a result, the site investigation and remedial action are subject to the requirements and regulations of the Comprehensive Environmental Response and Emergency and Liability Act (CERCLA). The Department of Defense (DOD) formulated and organized the Installation Restoration Program (IRP) to address investigation and remediation efforts as a result of hazardous waste disposal sites at DOD facilities. Through the Air Force Engineering Service Center, the NGB entered into an IAG with the U.S. Department of Energy (DOE). The NGB, with support of DOE, analyzed the extent of contamination and potential site contamination at the MMR facility (Bosch et al. 1996).

2.3.3 History of The Contamination And Cleanup-Up Efforts

The source area of Fuel Spill-12, is at the intersection of Greenway Road and the western entrance of the live firing range, about 3,000 ft north of Snake Pond. At this site, leakage from an underground fuel pipeline during 1965-72 resulted in a lens of free phase product floating on the water table and contaminated ground water as far as 5,000 ft down gradient from the contamination source area (Masterson et al. 1996). The pipeline was constructed in the early 1960s; its main purpose was to transport aviation fuel from the Cape Cod Canal to the National

Guard flight line area. Both aviation gasoline and JP-4 jet fuel were carried in the pipeline. The IRP has estimated a spill volume of approximately 70,000 gallons (Bosch et al. 1996). Because of their known carcinogenicity the contaminants of greatest concern in this plume include benzene and ethylene dibromide (EDB). The general direction of the plume movement is south-southwestward. The leading edge of the EDB plume is about 3,800 ft beyond the MMR base boundary and ranges in altitude from about 50 to 125 ft below sea level (Masterson et al. 1996).

3. Fuel Spill 12 Description

3.1 Physical Characteristics

3.1.1 Geology

The FS-12 site is located entirely in the Mashpee Pitted Plain (MPP). The geology of the site is typical of the MPP. Data indicate that the substrata consist of outwash sands and gravel with discontinuous lenses of fine sand, silt, and clay down to at least a depth of 130 feet below the water table. Engineers have not drilled to the bottom of the aquifer, so they can only guess as to the nature of the confining layer. There are two views in this regard: (1) The majority of the aquifer is confined by a deep clay layer, (2) The confining layer is bedrock. The bedrock has been mapped by using seismic surveys that produced data that appear to point to the bedrock as the confining layer.

A zone of surface soil and weathered residuum of approximately two to five feet is common in the study area. The interval typically consists of silty clay or clayey silt, with variable mixtures of fine sand and/or organic matter. Underlying this layer is the upper sand and gravel outwash deposits of the MPP. The substrata are unconsolidated and typically consist of sand with minor amounts of gravel. The sand is dominantly weathered quartz with some feldspar, the grains are typically poorly graded, mostly medium grained, and sub-angular to sub-rounded. The gravel component typically ranges between 0 to 25 percent of the lithology. The gravel is well graded, with clasts ranging in size from fine gravel to cobbles and boulders. The clasts are dominantly weathered granite. Locally, an abundance of coarse gravel is common in the uppermost 30 ft. The primary source bedrock for the outwash sediment appears to be granite. Below the uppermost 130 ft of the sand and gravel deposits, intervals of fine grained sediments were noted, particularly at depths ranging between 130 ft to 215 ft. Most intervals have not been penetrated, therefore thickness data are limited. The few borings that have penetrated these sediments of fine sand and silt show

3.2 Remedial Activities

There are two distinct remediation objectives: plume containment and source remediation. A proposed pump and treat (P&T) system, due to operate in the summer of 1997, will contain the plume. And air sparging (AS), in conjunction with soil vapor extraction (SVE), are currently being used to remove fuel at the source.

3.2.1 Plume Containment

The primary focus of plume containment will be to avoid impacts to Snake Pond. A P&T system has been designed based on a model of groundwater flow in the region of interest. An extraction and injection well fence system will be employed. Thirty preliminary extraction and injection wells are currently being installed. Data obtained from these wells will be used to refine and calibrate the model. The refined model will be used to decide the quantity and location of additional extraction and injection wells, and corresponding flow rates. The entire process is expected to take one-half to two years.

3.2.2 Source Remediation

An air sparging system and a soil vapor extraction system are currently in operation to remove fuel at the source of the FS-12 plume. Soil vapor extraction involves extracting air from the vadose zone via a vacuum pump. The idea is to take advantage of the high volatility of organic carbon compounds in fuel to remove the gasoline vapors above the free floating product. The removal of these vapors, in turn induces more of the liquid gasoline to vaporize vapor. This vapor is continuously removed by the SVE system.

Air sparging involves the injection of air into the saturated zone. Remediation occurs via two mechanisms: stripping and biodegradation. As the air moves upward and comes in contact with free or dissolved fuel, it strips the fuel from contaminated water and free product. As with

SVE, some of the fuel in the liquid phase becomes vapor when it comes in contact with the injected air and is carried off with the rising air. When the air reaches the vadose zone, it is extracted by the SVE system. Also, injecting air into the saturated zone supplies oxygen to fuel eating bacteria that break down the fuel to carbon dioxide and water. The SVE system began operation October 23, 1995. The AS system began operation February 21, 1996. As of September 22, 1996, an estimated 39,100 pounds of product had been removed from the site.

4. Natural movement of LNAPL in the saturated and unsaturated soils

(After - Cheremisinoff, 1986)

It is very important to understand how LNAPL behave in the subsurface. The transport mechanisms are often very complex as the behavior of chemicals in the subsurface are governed not only by their physical and chemical properties but also by the characteristics of the soil and rock formations through which they move.

Analyzing the fate and transport of LNAPL in the subsurface is a particularly complicated process because LNAPL are often a complex mixture of chemicals. Each compound found in the LNAPL has a unique set of physical and chemical properties that determines its multiphase flow characteristics. Therefore, it is often very difficult to determine how LNAPL will behave as a whole and the extent to which they will migrate in the soil and rock formations.

In the case of a large spill, the dynamics of the plume movement usually follow the pattern showed on figure 4. The LNAPL flows downward from the surface leaving in its path some residual saturation. With time, evaporation of the lighter components will create a gas zone around the LNAPL zone. Then, when the spill reaches the water table it will depress it and spread on top of it, dissolving its soluble components directly into the aquifer, thereby creating a plume of contaminated water.

The subsurface structure will greatly influence the way in which LNAPL moves in the underground. We can distinguish three main subsurface zones: the unsaturated zone, the capillary zone, and the saturated zone. In each of these zones, LNAPL components can move as solutes in the water phase, as free product, or as vapor in the air phase. Multiphase flow is further complicated because each subsurface formation has different characteristic properties which govern the transport of substances through it.

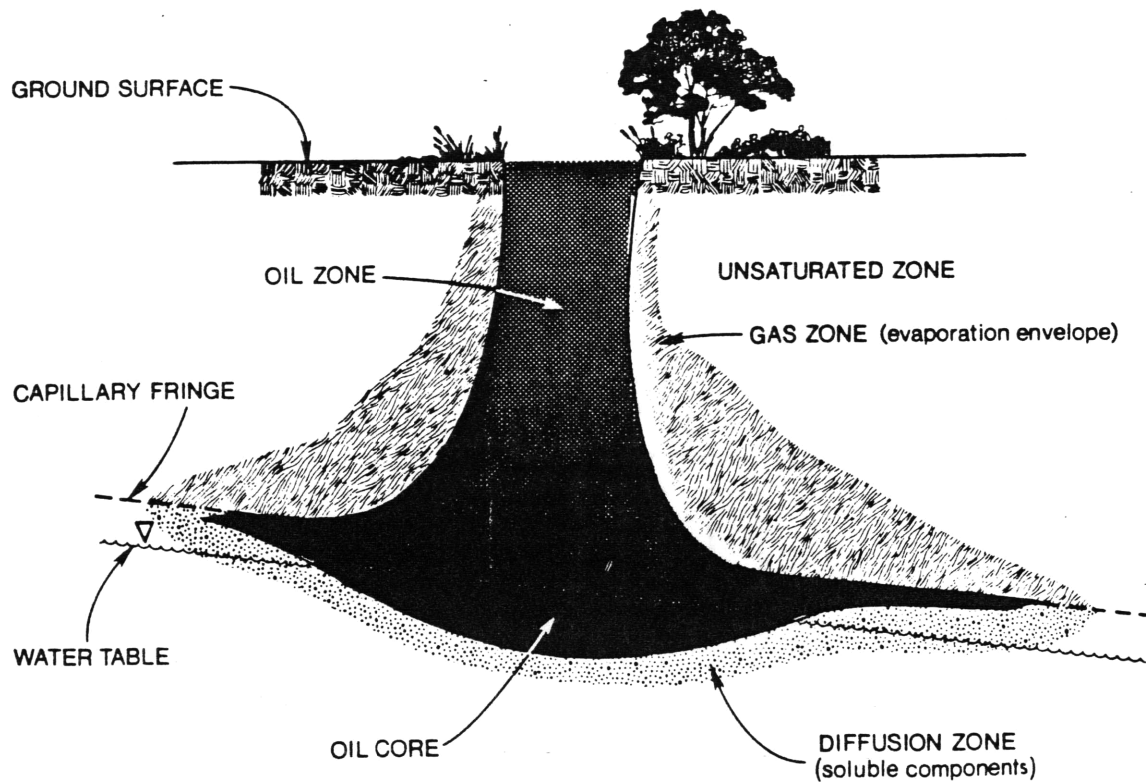


Figure 4: An Oil Seepage Schematic

(Abriola, 1984)

4.1 The unsaturated zone.

The unsaturated zone is the region that extends between the ground surface and the top of the capillary zone. Fluids can be retained there by absorption on the surface particles and by capillary forces (suction). The maximum amount of fluid that can be held in the pores by adsorption and capillary forces is referred to as the residual saturation. It is the threshold content below which the fluid is no longer able to move.

If the soil and product properties are known, whether the product will reach the ground water can be estimated. The following formula provides a useful approximation of the depth of migration for hydrocarbons:

$$D = R_v \sqrt{V / A} \quad 1$$

where D = maximum depth of penetration, m

V = volume of infiltrating hydrocarbons, m^3

A = area of spill, m^2

R_v = constant reflecting the retention capacity of soil and viscosity of product. It is a dimensionless, as is the residual saturation (m^3_{LNAPL} / m^3_{soil})

As LNAPL move into the soil, they migrate both vertically and horizontally. The vertical component is due to gravity while the horizontal movement is due to capillary forces. Migration occurs by successive permeation of larger area. In a highly permeable homogenous formation or with very dense fluids, gravity will take over and migration is mainly downward. In a less permeable formation, capillary forces will have a greater importance and the migration will be more horizontal. Migration in a heterogeneous soil formation will result in a complex succession of wide and narrow flow paths.

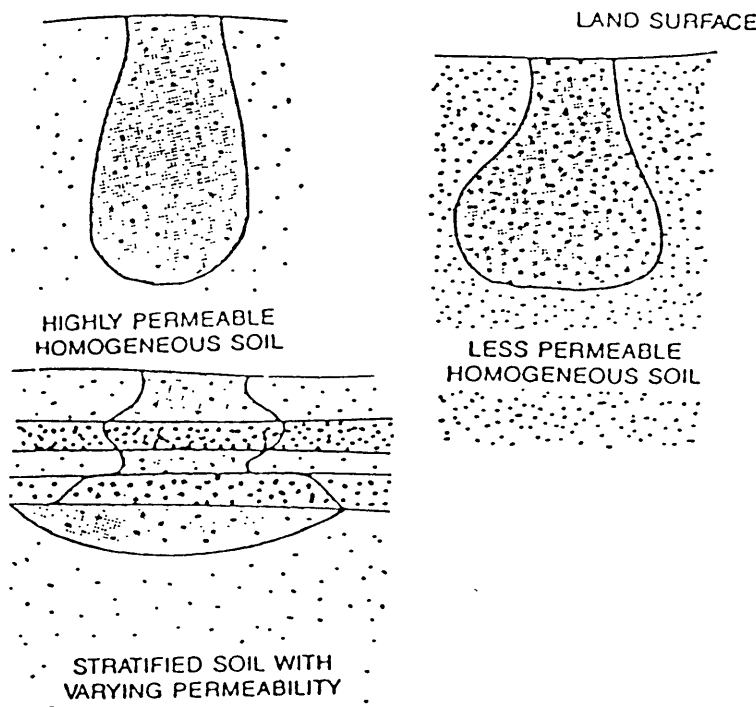


Figure 5: Contamination Transport Through Unsaturated Homogeneous And Heterogeneous Soils. (Cheremisinoff, 1985)

The vertical penetration of LNAPL in the unsaturated zone can be impeded in three cases

- when the saturation falls below the residual saturation (occurs when all the LNAPL is adsorbed to soil or rock particles or, is trapped in capillary spaces);
- when an impermeable layer exists in the path of the LNAPL (migration is then lateral until residual saturation is reached or until it reaches a discharge point or the edge of the impermeable layer);
- when the LNAPL reaches the water table.

4.2 The capillary zone.

The capillary zone is the transition between the unsaturated zone and the saturated zone. Moisture content in the capillary zone ranges from residual water saturation near the unsaturated zone to complete saturation at the water table.

When free LNAPL reaches the capillary zone, its vertical migration is stopped. As more LNAPL descends, a layer of increasing thickness forms and hydrostatic pressure is exerted, causing a local depression of the water table. As buoyant forces act to restore the original water level, lateral movement begins and a lens of gasoline forms and spreads out. Lateral spreading occurs in all directions, but the predominant movement is with the slope of the water table. Heterogeneity and permeability differences often influence the direction and extent of free LNAPL migration in the capillary fringe. In heterogeneous soils, LNAPL migration is along the path of least resistance. Soil permeability affects the rate and thickness of lateral spreading. In low permeability soils, resistance to flow is high and a thicker lens will be formed; lenses formed in higher permeability soils are thin and fast moving.

As in the unsaturated zone, transport in the capillary zone is governed by multiphase flow phenomena. The increased water content in the capillary zone affects the rates of volatilization and dissolution. As soil water content increases, volatilization and vapor transport generally increase. Free product migration occurs on top of the water table, and as the gasoline continues to spread, some of it gets captured by capillary trapping. When the free LNAPL is exhausted, migration stops and residual saturation is reached.

4.3 The saturated zone.

The saturated zone is the region below the unsaturated zone and the capillary zone where the pores are completely saturated with water.

When the LNAPL gets down to the water table it will tend to spread on the surface as buoyancy forces prevent it from moving down into the saturated zone. Once the LNAPL have reached their maximum extent, the free portion will be held in place by capillary forces. The only contaminant movement will therefore involve the dissolution of the LNAPL in ground water and the migration of the dissolved LNAPL compounds. Dissolved compounds get into the aquifer waters in several ways:

- Infiltrating water passes through LNAPL bound in the unsaturated zone and leaches some compounds and carries them to the aquifer.
- Free LNAPL can dissolve directly and moves with the groundwater as a single phase

Free product held as residual saturation in the unsaturated zone can be submerged by a rise in the water table. Capillary forces binding the submerged gasoline to the soil and rock particles will resist buoyant forces pushing the LNAPL up toward the elevation of the new water table. As a result, the LNAPL will remain in the saturated zone, and dissolution will occur freely. These mechanisms of capillary trapping are responsible for the poor results of the attempts to pump out free LNAPL.

5. Mechanism of LNAPL trapping in the saturated zone.

(New Mexico Institute of Mining and Technology, 1989).

There are three major forces acting in both oil recovery and organic liquid behavior in groundwater: capillary forces, viscous forces, and gravity or buoyancy forces. Capillarity is the result of the interplay of cohesive forces within each fluid phase, and the adhesive forces between the solid phases and the different fluids. The capillary force is proportional to the interfacial tension at the fluid-fluid interface and to the strength of fluid capacity. It is inversely proportional to the pore size. Viscous or dynamic forces are proportional to the permeability and to the pressure gradient, while buoyancy is a gravitational force proportional to the density differences between the fluids. For multiple fluid phase flow in an aquifer at typical aquifer flow rates, capillary forces often dominate over viscous and buoyancy forces. As we shall see, it is the dominance of capillarity that mainly causes the trapping of LNAPL.

To see how capillary trapping affects LNAPL we start by assuming that LNAPL first saturates the porous media and is later displaced by water. This is what happens in a typical case of LNAPL trapping in the soil; the LNAPL flows down to the water table and spreads over it. Then, at some later time, the water table rises, due to recharge or seasonal fluctuation, and the water progresses through the medium trapping some of the organic liquid as residual. The two major mechanisms of capillary trapping are snap-off and by-passing.

5.1 Snap-off

Snap-off occurs as non-wetting fluid in a pore is displaced from the pore body into the pore throat. As water is more wetting than LNAPL, the contact angle it makes with the pore walls is acute (less than 90°). When the water progresses in the pore it “creeps” along the walls until it reaches to the pore throat. As the waters leading edge enters the throat, it separates the free fluid remaining in the pore from the retreating fluid.

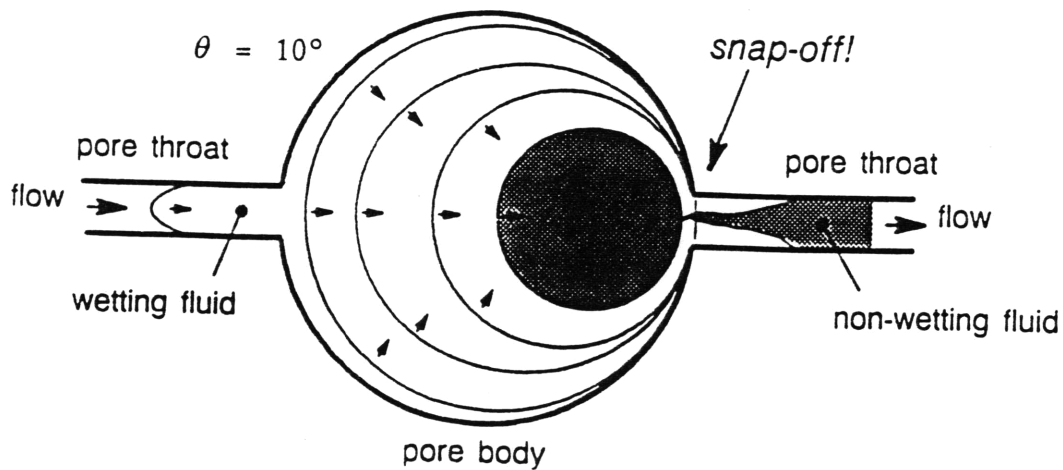


Figure 6: Wetting Fluid Displacing A Non-Wetting Fluid From A Circular, High Aspect Ratio Pore Under Strongly Wet Conditions.

(New Mexico Institute Of Mining And Technology, 1989)

From figure 6, we can see that the snap-off mechanism will be very dependent on the wetting condition and on the pore aspects. Figures 7 and 8 show how low wetting condition or a low pore aspect ratio can prevent snap-off.

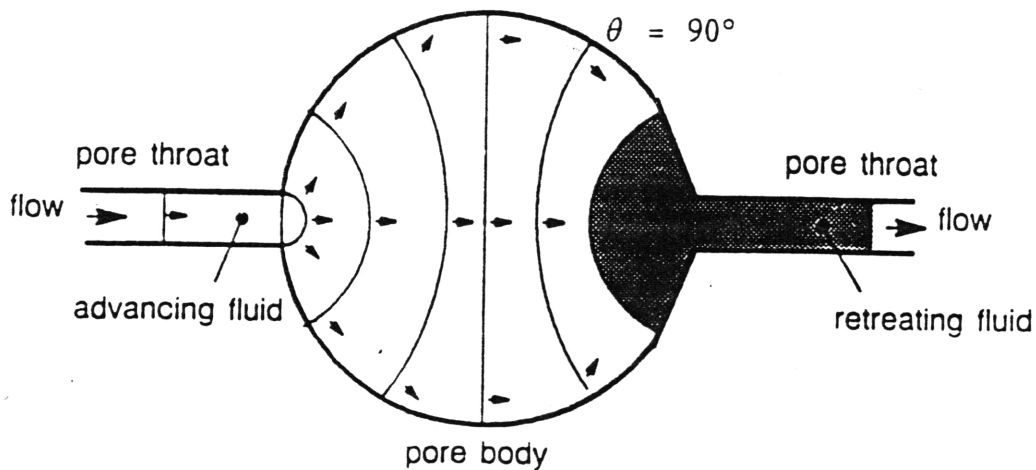
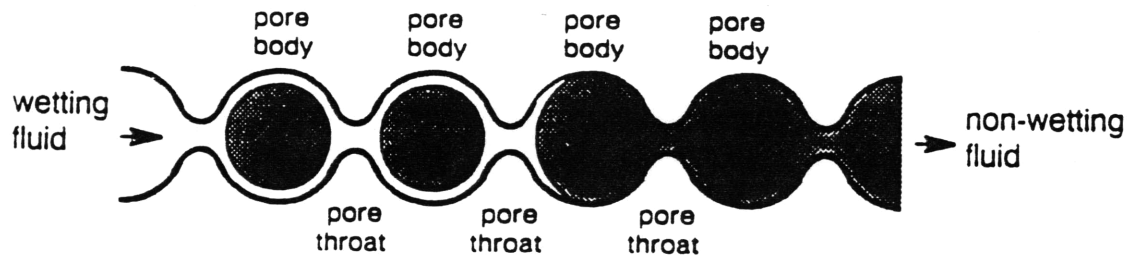


Figure 7: Low Wetting Condition.

(New Mexico Institute Of Mining And Technology, 1989).

a. high aspect ratio pores (snap-off):



b. low aspect ratio pores (no snap-off):

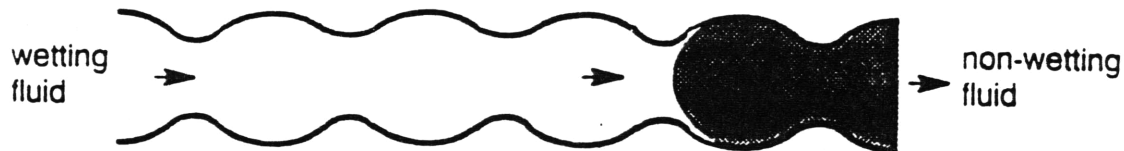


Figure 8: Effect of pore aspect ratio on LNAPL trapping.

(New Mexico Institute of Mining and Technology, 1989).

5.2 By-passing

To explain by-passing mechanism we use the pore doublet model. A pore doublet consists of a tube which splits into two pores, one generally smaller than the other, and then rejoins.

By-passing occurs when the flow rates are low enough to allow the capillary forces to be much larger than viscous forces. Capillarity then controls the advance of the wetting fluid as it displaces the LNAPL. The water therefore moves forward much faster in the narrower tube, and the water-organic interface remains stable at the entrance of the wider tube. When the water reaches the downstream node (where the pores rejoin) two things can happen:

- it forms a stable meniscus with the organic liquid if the cross-section at the downstream node is greater than the entrance to the wider pore. Water can then push the LNAPL out of the wider pore. → NO trapping (Figure 9 a)

- as no stable interface is formed, it does not stop. The organic fluid in the wider pore has become disconnected from the main body of LNAPL and is now unable to drain from the pore Figure (9 b).

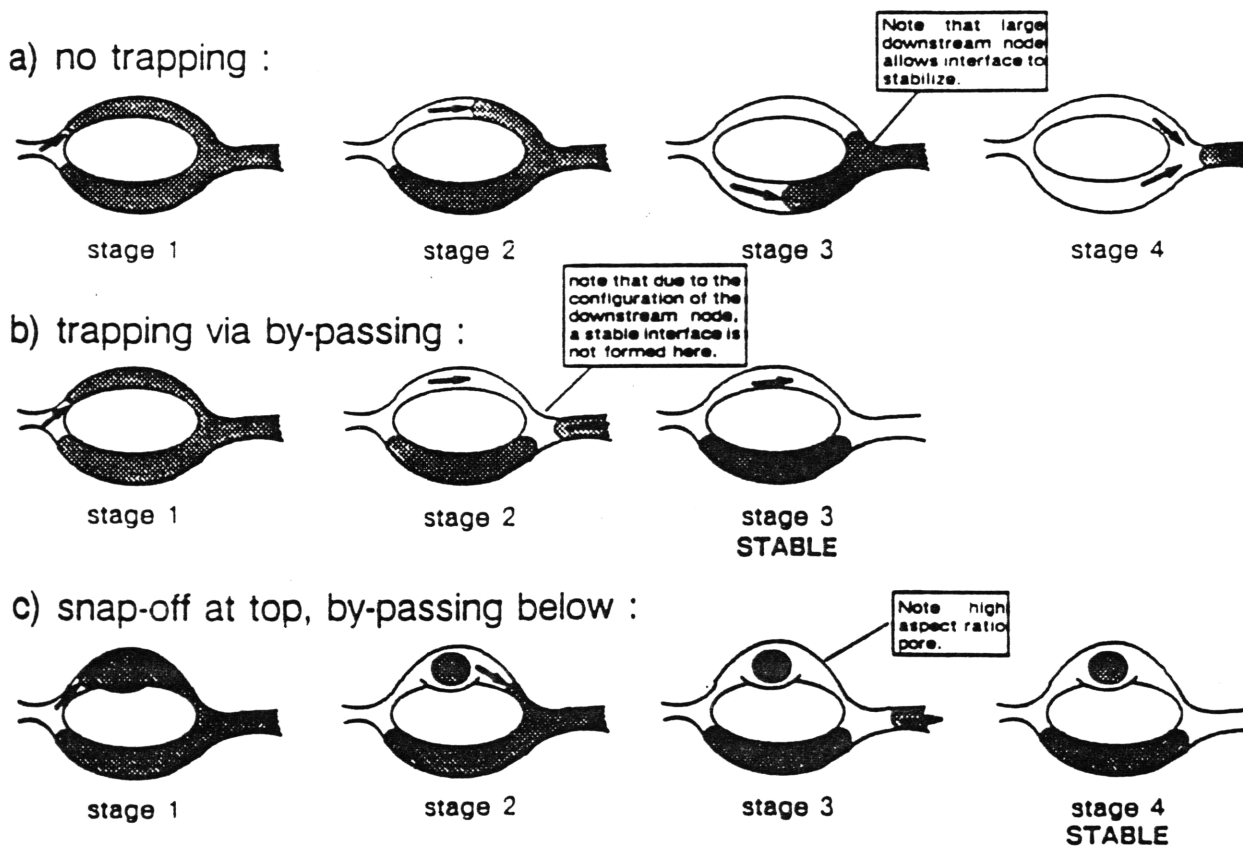


Figure 9: By-Pass Trapping Using The Pore Doublet Model.

(New Mexico Institute Of Mining And Technology, 1989).

6. Sound Waves And Ultrasounds For The Mobilization Of LNAPL

Two techniques are to be used at the FS-12 site: a pump and treat system that is proposed, and an air sparging system and soil vapor extraction which is already in operation. We think that both these systems could be complemented with the use of ultrasound. The pump and treat scheme is only a containment technique and is not capable of final clean up. The current scheme is focused on capturing the down-gradient plume.

To effectively treat the FS-12 source area an air sparging / vapor extraction remediation scheme was designed for the site. Air sparging flushes the LNAPL out of the saturated zone by bubbling air through it. The vapor is then captured in the unsaturated zone by soil vapor extraction. The vapor is in turn treated by passing it through an activated carbon filter. The combination of techniques is very cost effective when the level of LNAPL residual saturation is low but it loses its advantages as the residual saturation increases. When the evaporation rate of the LNAPL is low, then remediation time increases dramatically with the total mass trapped in the subsurface environment. To reduce the remediation time, it is therefore very important to pump as much free phase organic pollutant before starting an air sparging treatment. The interactions between the three phases - air, water, and LNAPL - and the geometry of the porous medium, combine to trap the pollutant in the subsurface, thereby preventing efficient pumping. At present two techniques are used to counteract the capillary trapping of free phase LNAPL: surfactants and direct flushing.

The direct flushing method is based on the brute force approach. The pressure gradient in the aquifer is increased by forcefully pumping water out of the aquifer and reinjecting it under pressure in a nearby well creating a strong pressure gradient. The LNAPL is thereby physically flushed out of the system. Unfortunately, this approach is seldom successful as the gradient needed to flush the LNAPL increases dramatically as the pore size diminishes. The cost of building injection and pumping wells at interval small enough to get significant pressures is often prohibitive.

Surfactants have been used for many years in the field of oil recovery. In the event of a water flood, capillary trapping can greatly reduce the amount of economically recoverable oil. Over the last twenty years, great progress has been made in oil recovery techniques using changes in miscibility and interfacial tensions. It is only recently, however, that the use of surfactant has been used in the frame of groundwater remediation. Two very different technical approaches utilizing surfactants are being considered: solution of contaminant into surfactant micelles and mobilization of residual liquids by reduction of the capillary forces trapping the liquid droplets in the aquifer porous medium (Harwell, 1992).

Over the past few years these two methods have had some success but they present their own problems. First, on a public perception level, the use of surfactant is often frowned on by the general audience and some regulatory agencies as they fear that the quality of the drinking water will be further jeopardized by the injection of new chemicals in the groundwater. Second, on a more technical level, it is often very hard to equally distribute the surfactant in the subsurface. Due to the high cost of building and maintaining injection wells, the remediation teams have to count on naturally occurring dispersion to bring the surfactant to the parts of the aquifer that are situated far from the injection wells. Moreover, with the lack of information that characterizes the subsurface environment, the placing of the injection wells and the modeling of the fate and transport of the surfactant can be a very difficult.

Realizing the limitations of the two previous techniques, we looked for a new approach to this problem. Our goal, here, is to evaluate if ultrasound can be used effectively to mobilize trapped LNAPL. We will therefor study the effects of ultrasound on trapped LNAPL on three scales.

On the molecular level. The high local pressures and temperatures created by ultrasound cavitation effects, can induce the chemical breakdown of the LNAPL. The molecular agitation created by cavitation effects of the ultrasound will also enhance molecular diffusion, thereby increasing dissolution. The higher breakdown and dissolution rates obtained by the application of ultrasound should dramatically shorten the time necessary to remediate the FS-12 site.

On a pore scale level. Use the energy of ultrasound to break down free floating bubbles of LNAPL. Breaking down these bubbles of free floating fluid into a fine emulsion will have two positive effects (Figure 10) . First, viscous forces will cause LNAPL to flow to the pumping wells in the form of free floating microbubbles that behave like colloids. Second, it will help the dissolution process of the LNAPL in the water by increasing the surface to volume ratio of the LNAPL bubbles. Combined with the use of surfactants, this technique could boost the free phase recovery in the capillary and saturated zone, and at the same time, increase the solution rate thereby considerably shortening the remediation time.

On the scale of a few pore lengths. The strong vibration induced by sound waves as they propagate through the porous media should cause transient conformational changes in the pore structure. These changes combined with the strong gradient caused by local pumping should be able to flush out LNAPL that would otherwise be immobilized by by-passing effect.

7. Background on the physics of ultrasound.

7.1 The production of sound wave and ultrasound.

Using a whistle equipped with an adjustable resonant cavity, Galton (1883) was the first to determine the lower limit of the ultrasound frequency range. Working on a large number of people he noticed that most of his subjects were not able to hear sounds that had a frequency higher than 16,000 cycles per second. He therefore decided to class as ultrasound any vibration that occurred at a frequency over 16 kHz (1 Hz = 1 cycle per second).

Sonic sources are regularly used in the industry: magnetostriction based transducers and piezoelectric transducers and the sonic whistle that generates ultrasound by passing a gas or a liquid through an orifice or over a ledge. The electric and magnetic transducers have two main advantage over the whistle transducers. First, they have a much larger frequency range, going from 16 kHz to 130 MHz, instead of 25 kHz. Second, they can produce waves of different geometry, depending on the type of electric or magnetic fluctuation the transducer is submitted to.

The piezoelectric effect was first studied by the Curie brothers (1880), when they noticed that charges appeared on the surface of certain crystals when they were put under pressure. The polarity was observed to change when the applied pressure was transformed into a tension. In the same way, if a difference in potential is applied on the crystal, it will contract or expand depending on the charge distribution on its faces. It was only thirty years later that this effect would be used to produce ultrasound. Langevin was the first to proposed the use of a piezoelectric transducer to produce the ultrasound needed for the localization of enemy submarines by the French marine.

He used a rapidly oscillating voltage source to force the high frequency oscillation of the crystal, thereby creating a stable source of ultrasound. Working with different types of crystals (e.g. quartz, barium titanate, Rochelle salts, lithium sulfate, tourmaline) with different cuts and with different frequencies, he realized that each crystal had its own resonance frequency at which the transducer was able to produce ultrasound at a relatively low energy cost.

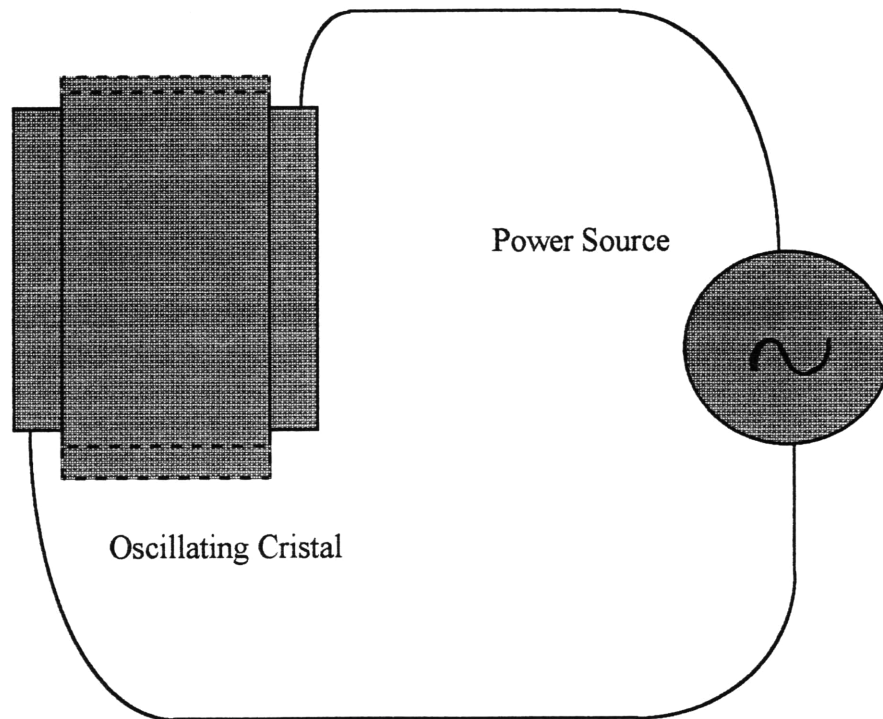


Figure 10: Piezoelectric Transducer.

Magnetostriction transducers work in a very similar way, but here ferromagnetic metals react to changes in a magnetic field instead of an electric field. Any material in a particular magnetic state can present only one combination of physical and chemical characteristics. So by changing their magnetic state, i.e. by applying an external magnetic field, we can change the physical characteristics of the metal (e.g. change its Young modulus). A periodic change in the magnetic field surrounding the metallic object will therefore induce a periodic change in the geometry of the object.

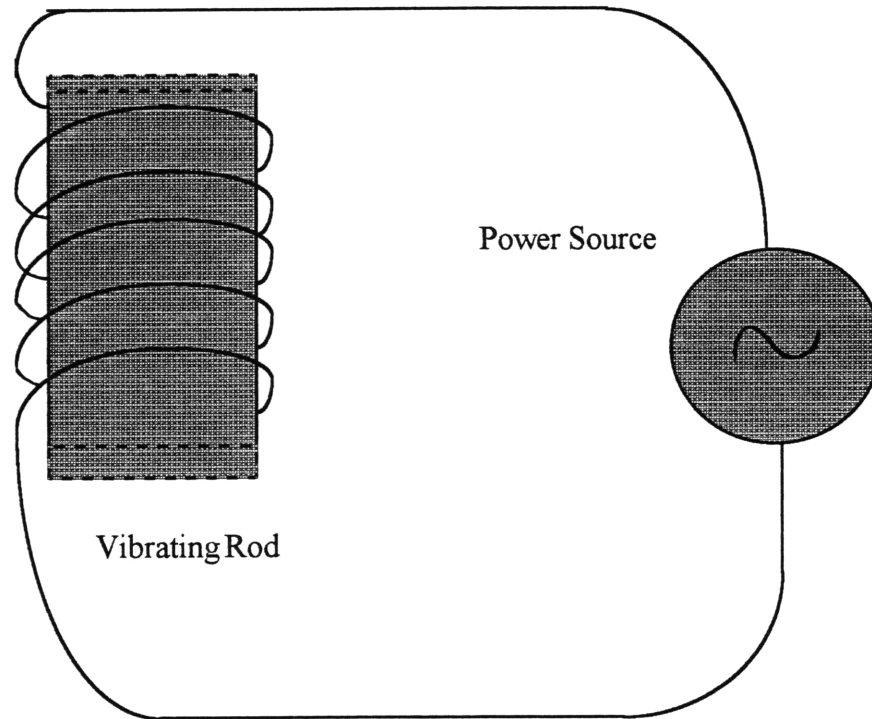


Figure 11: Magnetostriction Transducer

For the magnetostriction transducers, the resonance frequency depends on the length of the bar, the order of the harmonic, the modulus of elasticity and the density of the metal.

$$f = \frac{K}{2L} \cdot \sqrt{\frac{E}{\rho}} \quad 2$$

where f is the resonance frequency of the transducer,

K is the order of the harmonic

E is the modulus of the metal

ρ is the density of the metal.

L is the length of the rod.

The ferromagnetic metals that are principally use today in the magnetostriction transducers are iron, nickel, cobalt, and their alloys (Carlin, 1960). From eq. 2 we can see that if we consider only the first harmonic, magnetostriction will only allow us to produce ultrasound with frequency

lower than 60 kHz, as the length of the bar becomes too small when we try to further increase the frequency. Using higher harmonics, we can double or triple the frequency obtained but the efficiency rapidly drops with each rise in harmonic.

7.2 Propagation and physics of cavitation.

7.2.1 Ultrasound propagation

The ultrasound is a high frequency wave. Therefore it can propagate itself in any material that has elasticity. In the water, its wave length ranges from 10^{-4} inch at 500 mHz to 2.4 inch at 29 kHz. Its speed of propagation can be calculated by eq 3, which gives a speed of $1.43 \cdot 10^3$ m/s for an ultrasound propagating in water.

$$c = \sqrt{K/(\rho\beta_{is})} = \sqrt{1/\rho\beta_{ad}} \quad 3$$

where c : speed of wave in liquids

K : ratio of specific heat

β_{is} : compressibility at constant temperature

β_{ad} : adiabatic compressibility

Ultrasonic waves can be of two types, longitudinal waves, where the oscillating motion is in the direction of the propagation wave, or shear waves, where that oscillation is perpendicular to the direction of the propagation of the wave. In a liquid phase, the ultrasound can only exist in the longitudinal form.

Each time an ultrasound would encounter a barrier (e.g. solid/water interface or water/LNAPL interface) it can be reflected, reflected, or partially reflected and partially transmitted. Also, the transmitted wave can be refracted and change direction or change wave type. Finally, a wave passing through a small opening can be diffracted, and act as a new point source.

As we can easily see, it quickly becomes impossible to determine the exact path of an ultrasound in porous media saturated with multiple liquid and gas phases. It is however possible to treat the porous media as a homogenous media with some particular properties. For a complete discussion of the propagation of high and low frequency waves in a saturated porous media, we recommend the work of M.A. Biot (1956).

The main points that we can learn from that discussion are that:

- the dispersion of the ultrasound is practically negligible in the porous solid.
- the phase velocity of the wave is directly proportional to its frequency.
- the attenuation factor, or absorption factor is proportional to the square of its frequency.

Looking for a way of determining the porosity of a media by ultrasound investigation, Adler (1985) came up with an empirical relation between the attenuation of ultrasound and the porosity of the solid through which it propagates (eq. 4).

$$A(k,z) = A(k,z_1) \exp(-(3/4) (c/a_p) \text{gama}(ka_p)) \quad 4$$

where c is the volume concentration pores

a_p is the average pore radius

k is the inverse of the wave length.

$\text{gama}(k_{pa})$ is the reduced scattering cross section.

In his work on contact surfaces between grain in random granular media Tavossi (1993) introduces the relation between effective stress and ultrasound propagation. The main result of his research was to show a direct relation between effective stress and sound propagation velocity. He also noted that dispersion and attenuation decreased with a higher compression.

7.2.2 Cavitation.

Most of the molecular scale effects of ultrasound in water can be traced back to the same origin, the cavitation of water. Cavitation can be defined as the formation and collapse of transient microbubbles that are formed by the passage of a high intensity pressure wave through the liquid media. Cavitation was first characterized by Sir John Thornycraft and Sidney Barby at the turn of

the century (Mason, 1990). Their task was to investigate the poor performance of a new screw driven destroyer (*H.M.S. Daring*). They eventually traced the problem back to an incorrect setting of the propeller blades; the blades were set at too steep an angle, thereby causing very high tensile forces to appear behind the rapidly turning blades. These tensions were high enough to result in the “tearing apart” of the water, which greatly reduced the thrust of the propeller. Moreover, the rapid collapse of those cavities during the compression phase that follow the passage of the blade can give rise to extremely high local pressure and temperatures. These pressures were of the order of 1000 atm and the temperatures could climb to 5000 °K during the collapsing phase of the bubble. It is easy to see that even propellers made of the toughest copper alloy will suffer extensive damage in those conditions.

The same cavitation effects can also be created by the irradiation of water with a high energy ultrasound. To understand the physics behind the cavitation induced by ultrasound it is very useful to compare the source of the ultrasound to a small piston immersed in water. During the compression phase, the piston advances and pushes the molecules of water in front of it, thereby creating a zone of high pressure. Then, during the decompression phase, the piston moves back to its original position, exerting a suction force on the water molecules directly adjacent to it. In the case of ultrasounds this cycle is repeated more than 20,000 times per second. The pressure wave that is associated with the propagation of ultrasound in water is given by eq. 5.

$$P_a = P_A \sin \omega t + P_h \quad 5$$

where, P_a is the local pressure, P_A is the maximum compression pressure, P_h is the local hydrostatic pressure, and ω is the angular frequency of the wave. A cavitation bubble will form during the rarefaction cycle if the net negative pressure applied to the liquid exceeds the cohesion force of the liquid. When the distance between the molecules exceeds the critical molecular distance necessary to maintain the integrity of the liquid, it breaks down and a void is created i.e. a cavitation bubble is created. The critical distance for water being 10^{-5} cm, the tensile stress or pressures involved can be calculated to be of the order of 10 000 atmospheres ($P_a \sim 2\sigma/R$ where σ = surface tension) (Mason, 1990). This however, assumes that the water is completely pure. Small impurities, or preexisting microbubbles, by creating weak spots in the liquid lattice, will greatly reduce the pressures needed to break down the inner cohesion forces.

The bubbles formed during the rarefaction phase are subjected to a sharp rise in external pressure during the next compression phase. If their radius is smaller than the critical radius, they will collapse, with the production of very high local pressures and temperatures (Blitz, 1967). The critical radius, R_o , corresponds to the radius of the smallest bubble that can survive the compression cycle. It can be calculated using eq. 6 (Blitz, 1967)

$$\omega^2 R_o^2 = 3 \gamma / \rho (P_h + 2 \sigma / R_o) \quad 6$$

where ω is the angular frequency of the wave, γ is the ratio of the principal specific heat of the gas in the bubble, ρ is the density of the fluid, P_h is the hydrostatic pressure, and σ is the surface tension of the liquid. The magnitude of the energy released by the collapse of the cavitation bubbles is proportional to the ratio R_M/R_o where R_M is the maximum radius attained by the cavitation bubble.

Finally, the maximum temperature and pressure obtained during the collapse of a cavitation bubble can be calculated using eq. 9.7 and 9.8 (Blitz, 1967)

$$T_{\max} = T_o \{P_m/P_h (\gamma-1)\} \quad 7$$

$$P_{\max} = P \{P_m/P_h (\gamma-1)\}^{\gamma/\gamma-1} \quad 8$$

where P_m is the pressure in the bubble at its maximum expansion. P_m can be approximated by the vapor pressure of the liquid, T_o is the temperature of the liquid, P_h is the hydrostatic pressure, and γ is the ratio of specific heat for the gas.

By analogy with the electrical vibration it is considered that the intensity of the wave (I , the energy transmitted per second per meter square of fluid) is described as eq. 9 (Mason, 1990)

$$I = P_A^2 / 2 c \rho \quad 9$$

where P_A is the maximum acoustic pressure, ρ is the density of the medium and c is the velocity of sound in the medium.

As stated before, the pressure necessary to induce cavitation in pure water can be calculated to be of the order of 10 000 atm which, using eq 4&5 correspond to an intensity of 10^6 W/cm². When we look at the experimental curve of the evolution of the threshold intensity with frequency, we can see that at low frequency, we can have cavitation with intensity as low as 0.1 W/cm² (Figure 9.9).

This lowering of the cavitation threshold can be attributed to a series of different factors
(After Mason, 1990)

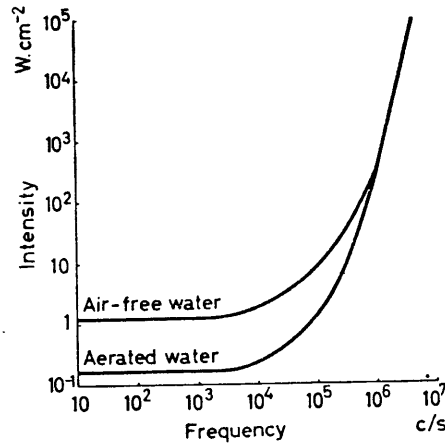


Figure 12: Variation Of Threshold Intensity With Frequency Of Water At Room Temperature

(Blitz, 1967)

Physical property of the solvent

Each solvent will have its own particular solvent parameters. The intermolecular forces within the liquid will greatly influence the cavitation threshold. Hydrogen bonds and van der Waals forces give cohesion to the liquid and any variation in the distribution of these forces due to dissolved salts or organic compounds will give rise to variation in the cohesion of the liquid. Surface tension is also very important in determining the cavitation threshold, a higher surface tension giving a higher cavitation threshold. The use of surfactants or other chemicals to lower the surface tension will therefore lower the cavitation threshold.

Temperature of the solvent.

Cavitation can be very sensitive to the solution temperature. As the boiling point of some of the dissolved compounds is approached, they will tend to boil during the rarefaction cycle. Any cavitation bubble formed will instantaneously fill with solvent vapor. The collapse of these vapor filled bubbles during the compression cycle will be “cushioned”, or even totally prevented.

Irradiation frequency.

In order to achieve changes in chemical reactivity the sonochemist will normally use frequency between 20 and 50 kHz. (Mason, 1990) The reason for this are twofold: first, most commercially available equipment operates within this range, and secondly it is more difficult to achieve cavitation at higher frequencies. To understand the problem involved in the production on ultrasound a very high frequency one must consider first that there will be a natural delay between applying a rarefaction wave to a fluid and this fluid responding. At frequencies in the megahertz range one must compensate for this delay by applying a wave of greater intensity - so that the effective pulling apart of the molecules is greater. Unfortunately it is almost an insurmountable engineering problem to drive a very high frequency transducer assembly at the vibration amplitudes (intensities) required.

Presence of dissolved gases.

When a cavitation bubble is initiated in the rarefaction cycle, it will not enclose a vacuum but will almost certainly contain some vapor of the liquid within which it is formed. It is clearly easier for that bubble to form if it is created in a solvent of high vapor pressure. In the limit, this vapor pressure would be so high that the liquid would boil into the bubble. The extent to which a gas is soluble in a medium depends upon the applied pressure; any sudden reduction of the this pressure will release the gas. It is therefore apparent that during the rarefaction cycle any gas dissolved in the medium will be forced out of the solution to form the nucleus of a cavitation bubble. From the equation 7 and 8 we can see that the ratio of specific heats of any gas in the bubble is a very important factor when considering collapse temperatures and pressures.

This is the reason why ultrasound can be used for degassing a liquid. Microbubble in a fluid saturated in a soluble gas would contain plenty of that gas. The presence of a large amount of gas would cushion and perhaps prevent the total collapse of the bubble in the succeeding compression cycle. The next rarefaction cycle would then attract more gas into the bubble, and so on. At 20,000 Hz the microbubble would rapidly achieve the status of an actual bubble within the liquid. At this stage the bubble would be buoyant, float to the surface and discharge to the atmosphere. As we can see this phenomenon could be used in parallel with soil vapor extraction.

Presence of particles.

Any particle present in the solvent will act as seed for cavitation. This can be done in two ways. First by disrupting the lattice of hydrogen bonds that give water its cohesion, particles can create weak spots that will break at lower tension. Second, particles can have entrapped gases in their crevices and recesses which readily become the nuclei for new forming cavitation bubbles (figure 13).

External hydraulic pressure

The cavitation threshold depends upon the rarefaction cycle generating pressure that can remove and exceed the ambient pressure on the system. Increasing the external pressure has the effect of increasing the cavitation threshold of the system by requiring a larger negative pressure in the rarefaction phase.

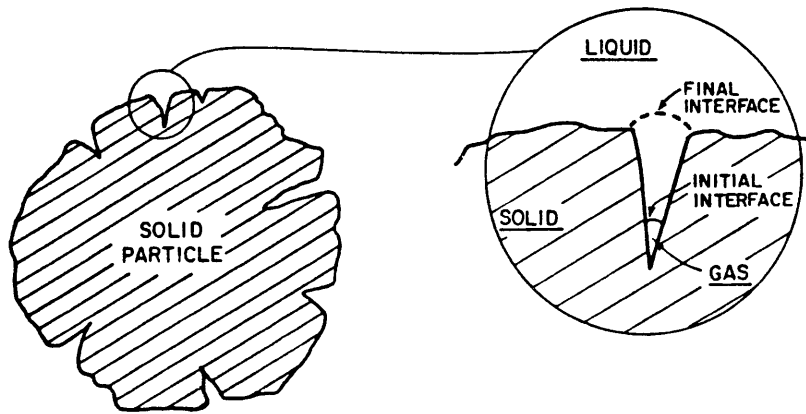


Figure 13: Microbubbles (10^{-6} cm) attached to free floating dust particles ($5 \cdot 10^{-5}$ cm)

Length of exposure to radiation

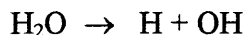
Every time a bubble that is created by cavitation collapses, the implosion is so strong that it tends to leave behind a few very small bubbles of superheated gas and vapor. These bubbles can then become primers for the formation of a new cavitation bubble during the next rarefaction cycle.

8. Effects of ultrasound on LNAPL in water.

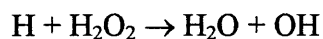
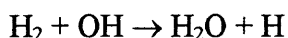
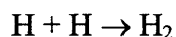
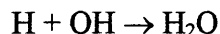
8.1 Molecular scale effects of the ultrasounds on LNAPL in water.

8.1.1 Effects of the ultrasounds on the chemical breakdown of LNAPL in water.

The use of ultrasound for the chemical break down of chemicals was first demonstrated in the 1950's. When cavitation occurs in water the resultant electrolyte action separates the H₂O molecule into H and OH radicals (Blitz, 1967),



This may be followed by one of the following reactions (Lindström and Lamm)



Therefore, ultrasonic irradiation of aqueous solution can be a useful method to investigate the reactivity of OH radicals which play important roles in environmental chemistry.

We will here summarize the finding of two recent studies of the decomposition of chlorinated hydrocarbons in aqueous solutions by ultrasonic irradiation. Their main interest lies in the fact that they attribute the break down of the structures not to the production of free radicals but to the high temperatures that are obtained during the collapse of cavitation bubbles. Inazu (1993) showed the rapid decomposition of trichloroethylene, tetrachloroethylene, 1,1,1-trichloroethane, chloroform and carbon tetrachloride to chloride anions, hydrogen, carbon monoxide and carbon dioxide by ultrasonic irradiation. The irradiation was carried out with a high intensity generator (200 kHz, 6W/cm²). As seen on Figure 14, over 75% of the initial amount in chlorinated carbon was decomposed after 10 min.

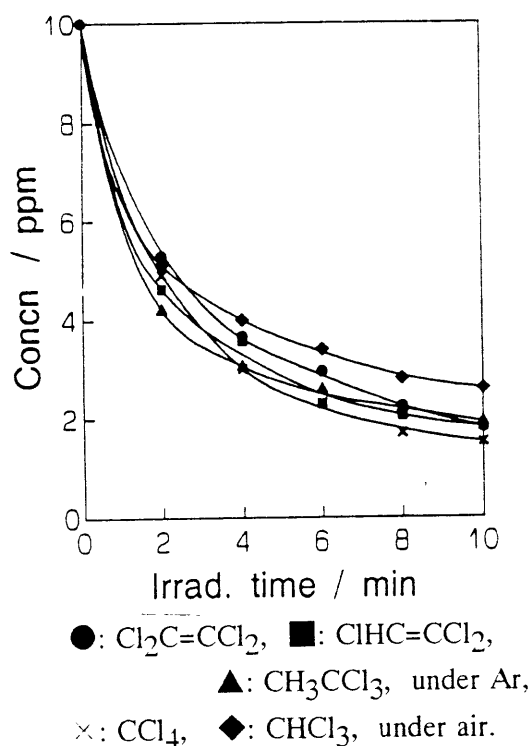


Figure 14: Time Profiles Of Five Chlorinated Hydrocarbons By Ultrasonic Irradiation

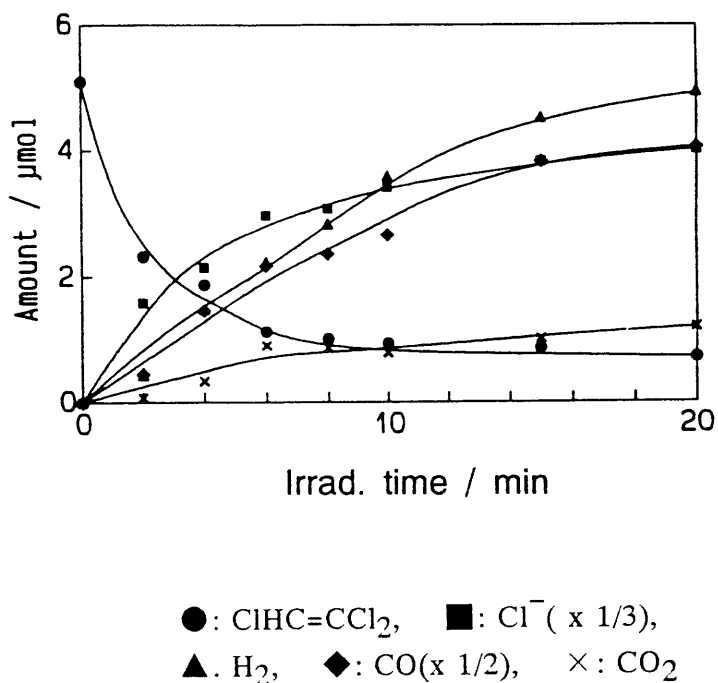


Figure 15: Time Profile Of Degradation Of Trichloroethylene And Transformation Of Products Under Argon.

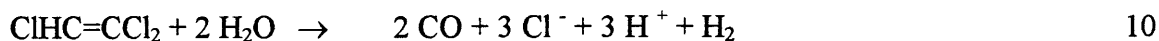
Three main reasons to reject the radical driven process

- The decomposition of trichloroethylene was not suppressed by the addition of tert-BuOH which is a known scavenger of OH radicals
- Sonolytic decomposition of 1,1,1-trichloroethane was about 5 times faster than γ -induced decomposition under N_2O (in which the OH radical is the main reactive species).

- The degradation rates in argon and oxygen were not very different, although H atoms would be quenched by oxygen and no hydrogen was formed in air or oxygen atmosphere.

The reactivity of the chlorinated hydrocarbons is attributed to their high volatility and their low solubility in water, properties which facilitates them to concentrate in cavitation bubbles and to decompose rapidly by pyrolysis at high temperature (Hart, 1986)

The two main reaction pathways that are proposed for the breakdown of trichloroethylene are shown in eq. 10 and 11.



Similar results were obtained by Cheung (1991). He observed the rapid destruction of methylene chloride, carbon tetrachloride, 1,1,1, trichloroethane and trichloroethylene, when solutions in the 100-1000 range were submitted to sonic irradiation in the range of 20-100 kHz.

8.1.2 Emulsification by ultrasound irradiation.

One of the most spectacular manifestation of the effects of the high frequency sound waves is their emulsifying action on benzene, paraffin and even mercury in contact with water. When benzene and water are placed in a test-tube which has been previously wet by water and the tube is irradiated with intense sound waves of 300 kHz, the benzene layer at once becomes cloudy, the water layer more slowly so, and, finally, the boundary between the two disappear (Richards, 1929). The emulsification of LNAPL with water can be attributed to two separate mechanism, microstreaming and the physical interaction between the two liquid phases and the wall of the tube containing them.

As we have seen, the sonic irradiation of a liquid produces transient bubbles by tearing the liquid apart during the rarefaction cycle. If these bubbles survive during a few cycles or become permanent, their oscillation can give rise to microstreaming. Microstreaming is the formation of very small flow of liquid in localized areas of the media exposed to sonic irradiation. Figure 16 gives an example of the flow field that appear in the vicinity of a oscillating air bubble as the

intensity of the sound producing the vibration increases. When microstreaming occurs near an interface between two immiscible fluids, a discontinuity may appear at the interface and the microstreaming of the two liquids merge, resulting in the emulsion of one liquid in the other.

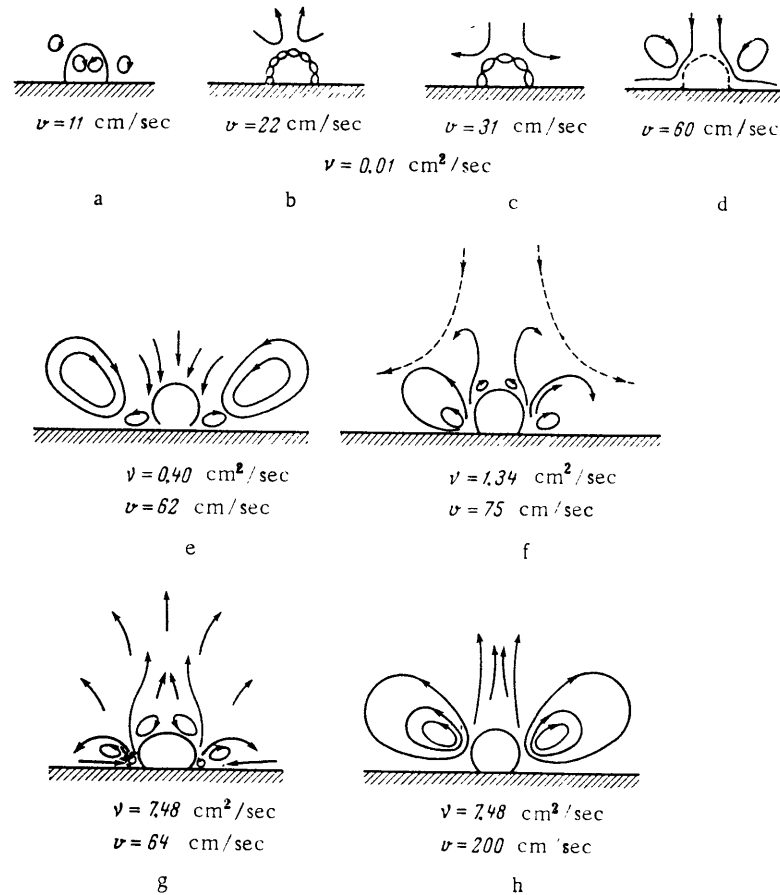


Figure 16: Microstreaming in the vicinity of oscillating air bubbles; v is the particle velocity of the bubble surface.

(Rozenberg, 1971).

Studying the emulsion of benzene and water, Richards (1929) noticed that when the test-tube containing the two phases was irradiated with sound waves of 300 kHz, the emulsion tended to be formed primarily along the walls of the tube and not at the center of the tube. He therefore concluded that, at low intensities, it was improbable that the longitudinal wave produced the

mixing action; more probably, it was the transverse waves in the glass that were the responsible agents.

As stated before, our interest in inducing the emulsion of LNAPL is two fold. First, by breaking down the LNAPL ganglia into micro-bubbles, we aim to prevent the capillary trapping of the LNAPL. The organic phase is then free to float to the surfaces of the aquifer where it can be pumped out. This could significantly boost the free phase product recovery, thereby considerably shortening the remediation time (Figure 17). Second, as the mass transfer of the LNAPL in the ground water is diffusion controlled and therefore independent of flow rate (Pfannkuch, 1984), increasing the exchange surface will shorten the remediation time. This could be achieved by the emulsion of the LNAPL as the smaller bubbles will have a larger surface to volume ratio.

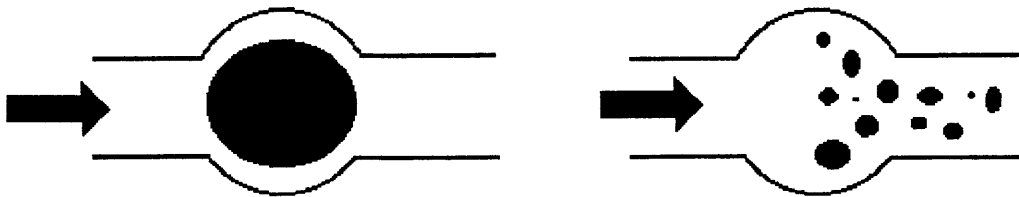


Figure 17: Effects of emulsification of LNAPL mobilization.

8.2 Effects of vibration on LNAPL mobilization.

The effect of vibration has been extensively studied by Lakshmi Reddi in a series of papers published between 1992 and 1996. In this section we will summarize the findings published by L. Reddi and H. Wu (1996) and go over the mechanisms involved in the vibratory destabilization of LNAPL ganglia in sand.

When submitted to vibration, the pore structure can experience transient or permanent pore structure changes. In the presence of LNAPL ganglia, these reorganizations can induce changes in the equilibrium between the capillary, viscous and buoyancy forces thereby allowing the LNAPL to mobilize. The criterion for ganglia mobilization can be expressed as (Reddi and Wu, 1996)

$$P_b + P_v > P_c \quad 12$$

These pressure component may in turn be expressed as (Reddi and Challa, 1994)

$$P_b = \Delta\rho \, g \, L \quad 13$$

$$P_v = \mu_w \, V_f \, L / k \quad 14$$

$$P_c = 4 \, \gamma_{ow} \cos \theta / d_t \quad 15$$

where γ_{ow} = interfacial tension between the immiscible liquid and water.

μ_w = dynamic viscosity of the aqueous phase.

V_f = Darcy velocity of the aqueous phase in the vertical direction.

d_t = diameter of pore throat containing the interface of the two liquids.

k = absolute permeability of the soil

$\Delta\rho$ = density difference between the water and the LNAPL.

g = acceleration due to gravity

θ = contact angle of the wetting fluid.

assuming that the contact angle is 0 and substituting (9.13), (9.14), and (9.15) in (9.12) yields and expression for the length (L) of a stable ganglion as

$$L = 4 \, \gamma_{ow} / (\mu_w \, V_f \, d_t / k + \Delta\rho \, g \, d_t) \quad (9.16)$$

The parameter d_t and k are affected by the pore structure changes due to vibrations. The sensibility of L to d_t was used to obtain the variation of the stable length of ganglion in figure 18.

As seen in figure 18 (a), the length of stable ganglia decreased as d_t is reduced. This is because, although a reduction in d_t in the denominator tends to increase the value of L , the decrease in k offsets this increase. In the presence of buoyancy pressure only ($V_f = 0$) however, the reverse trend is observed with the length of ganglia increasing as d_t is reduced (Figure 18 (b)). This difference between the effect of viscous and buoyancy forces can be explained by figure 19. The vibration causes the compacting of the media. In the absence of viscous pressure, this induces the elongation of the ganglia (Figure 19 (b)). In the presence of viscous pressure however, “snap-off” will occur and the ganglia will be reduced in size.

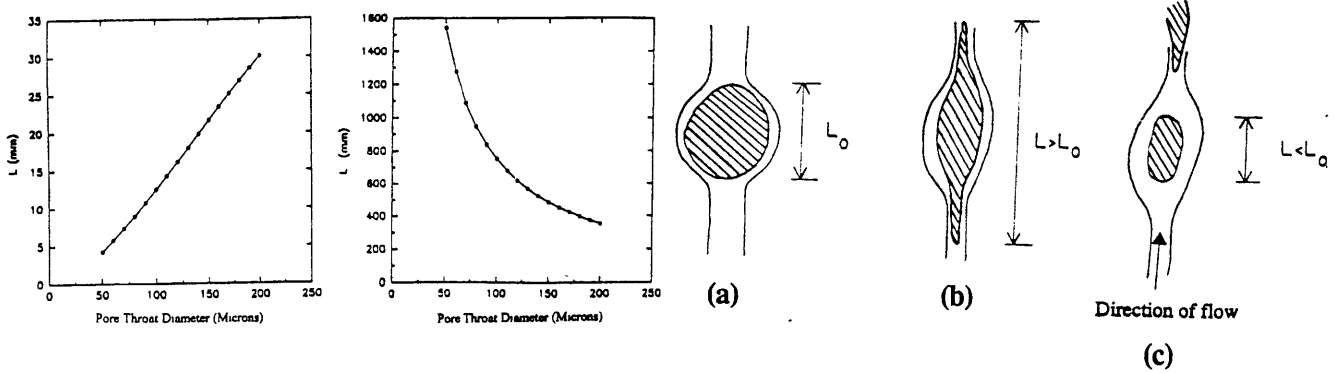


Figure 18: Theoretical variation of the maximum length of stable ganglion with respect to pore throat diameter under (a) viscous conditions; and (b) buoyancy conditions (Reddi and Wu, 1996).

Figure 19: Hypothesized changes in ganglion geometry :(a) stable ganglion under static conditions; (b) elongated ganglion due to change in pore structure under buoyancy pressure alone; and (c) split ganglion due to change in pore structure under viscous pressure (Reddi and Wu, 1996)

The predictions offered by this approach were usually consistent with results obtained in laboratory experiments. In some cases however, vibration can induce the recovery of substantial amounts of LNAPL even if there is no permanent changes in the pore structure in the media. This can be attributed to the initial period of vibration during which the particles are in the transient state of being reoriented and the pore throat dimensions momentarily change. Although the pore structure at the end of the vibration resulted in a compact arrangement, the transient nature of pore throat changes during vibration might enable a momentary release of ganglia.

9. Conclusion

As we have seen in this paper, the use of ultrasound in LNAPL remediation has great potential. Before being able to use this form of remediation we need to address a few key issues.

First, work will have to be done to determine to what extent cavitation will be affected by working with a liquid saturated porous media. As we have stated, cavitation is the basis of two of the three basic mechanism that make ultrasound a potential remediation alternative: the degradation of dissolved compounds and the emulsification of free floating bubbles of LNAPL. It is therefore of foremost importance to determine the threshold level of cavitation in liquid saturated porous media. By the same token, some work should be done to determine the attenuation factor of high intensity ultrasound in unconsolidated liquid saturated porous media. This would allow for the evaluation of the radius of influence associated with a ultrasound source of a determined intensity for a sandy aquifer having a known porosity.

Second, using vibration to cause the mobilization of trapped LNAPL, Reddi (Reddi et al. 1996) noticed that overburden stress had a considerable impact on the efficacy of the technique. If vibration is to be used in the field, with overburden stresses far greater than the ones encountered in laboratory sediment columns, this dependency needs to be better understood.

Third, test should be made to determine what wave lengths are optimum for each of the three remediation mechanisms.

And finally, if one of these technique is to be used in the field one day, some investigation should be made concerning the potential effects of high intensity ultrasound on the wild life. Some pest repelling ultrasonic devices can be found on the market and the potential negative effect on the ecology of the site under remediation should not be overlooked.

10. Reference.

- Abriola, Linda M. Multiphase Migration of Organic Compounds in a Porous Media - A Mathematical Model. Springer-Vellag, New-York. 1984.
- Blitz, Jack. Fundamentals of Ultrasonics. Butterworth, London. 1967.
- Biot, M.A. Theory of Propagation of Elastic Waves in a Fluid-Saturated Porous Solid. The Journal of the Acoustical Society of America. Vol. 28 No. 2 p.168. March 1956.
- Carlin, Benson. Ultrasonics. McGraw-Hill Book Company, Inc. New York. 1960.
- Cheremisinoff, Paul, N. Underground Storage Tanks - Evaluation, Site Assessment , & Remediation. McGraw-Hill Book Company, Inc. New York. 1986.
- Cheung, H.M., A. Bahtnagar, and G. Jansen, Environmental Science and Technology, **25**, 1510 (1991)
- J. Curie & P. Curie, *Compt. Rend.*, **91**, 294 (1880)
- Department of Environmental Management, Massachusetts Executive Office of Environmental Affairs. *Water Resources of Cape Cod*. October 1994.
- Galton, F. *Inquiries into Human Faculty and Development*. MacMillan, London, 1883.
- Hart, E.J., and A. Henglein, Journal of Physical Chemistry, **90**, 5992 (1986)
- Harwell, Jeffrey H. *Factors Affecting Surfactant Performance in Groundwater Remediation Applications*. In "Transport and Remediation of Subsurface Contaminants" by Sabatini, David A. and Knox, Robert C.. American Chemical Society. 1992.
- Inazu, Koji, Yoshio Nagata, and Yasuaki Maeda. "*Decomposition of Chlorinated Hydrocarbons in Aqueous Solutions by Ultrasonic Irradiation*". Chemistry Letters. 1993.
- Mason, Timothy J. "Chemistry with Ultrasound", Critical reports on applied chemistry :v. 28. Elsevier Science Publishing Co., Inc., New York. 1990.
- New Mexico Institute of Mining and Technology, Scorro, NM. *Laboratory Investigation of Residual Liquid Organics form Spills, Leaks and the Disposal of Hazardous Wastes in Groundwater*. U.S. Department of Commerce, National Technical Information Services. Aug. 1984.

- Pfannkuch, Hans-Olaf, *Determination of the contaminant source strength from mass exchange process at the petroleum-ground-water interface in shallow aquifer system. Proceedings of the NWWA/API Conference on Petroleum Hydrocarbons and Organic Chemicals in Ground Water - Prevention, Detection and Restoration*. National Well Water Association. 1984.
- Reddi, Lakshmi and Hui Wu. *Mechanisms Involved in Vibratory Destabilization of LNAPL Ganglia in Sand*. Journal of Environmental Engineering, p. 1115, December 1996.
- Reddi, Lakshmi and S. Challa. *Vibratory Mobilization of Immiscible Liquid Ganglia in Sand*. Journal of Environmental Engineering p.1170. 1994.
- Reichmuth, Dr. Donald R. *Subsurface Gasoline Migration Perpendicular to the Ground Water Gradient - A Case Study. Proceedings of the NWWA/API Conference on Petroleum Hydrocarbons and Organic Chemicals in Ground Water - Prevention, Detection and Restoration*. National Well Water Association. 1984.
- Richards, William T., *The Chemical Effects of High Frequency Sound Waves : A Study of Emulsifying Action*. Journal of American Chemical Society. Vol. 51 1724 (1929)
- Rozenberg L.D., High-Intensity Ultrasonic Fields Plenum Press. New York London, 1971
- Stone & Webster Environmental Technology & Services. *Final Record of Direction for Interim Action. Containment of Seven Groundwater Plumes*. 1995
- Tavossi, H. and F. Cohen-Tenoudji. Ultrasonic Investigation of Contact Surfaces Between Grains in Random Granular Media, Effects of Variable Compression. Ultrasonics International 93 Conference Proceedings. Vienna, Austria, July 1993.
- Wood, W.W., T. F. Kraemer, and J. Hearn. P.P. "Science", 247, 1569.